Nuclear Instruments and Methods in Physics Research A 379 (1996) 139–151

ELSEVIER

NUCLEAR INSTRUMENTS & METHODS IN PHYSICS RESEARCH Section A

Microchannel plate operation at high count rates: new results

A.S. Tremsin[a], J.F. Pearson[a], G.W. Fraser[a,*], W.B. Feller[b], P. White[b]

[a]*X-ray Astronomy Group, Department of Physics and Astronomy, University of Leicester, University Road, Leicester LE1 7RH, UK*
[b]*Nova Scientific Inc., 54 Main Street, 7 Cedar Court, Sturbridge, MA 01566, USA*

Received 26 April 1996

Abstract

We describe an experimental study of two distinct microchannel plate (MCP) detector configurations with extended dynamic range. First, we report on measurements made with single MCPs of very low resistance ($\leq$500 kΩ) bonded to a Peltier cooler. Stable, reproducible operation for a rear-cooled MCP with 10 μm diameter channels of length-to-diameter ratio 60:1 was achieved for biases up to 1320 V. At this point, the MCP strip current was 5.1 mA and the rate of internal heat generation, 0.78 W cm^{-2}. A maximum count rate of 10^8 cm^{-2} s^{-1}, limited by the available intensity of UV illumination, was observed, coupled to a dark noise count rate of less than 1 cm^{-2} s^{-1}. Second, we describe a substantial (up to 20-fold) improvement in count rate capability for two-stage MCP multipliers incorporating plates with gold, rather than nichrome, electrodes. We also present, in support of the experimental study, a thermal model of bonded, conductively-cooled MCPs which we use to determine critical parameters for stable detector operation.

1. Introduction

We have previously [1,2] studied the mechanisms limiting the high count rate operation of microchannel plane (MCP) electron multipliers. A simple paralysable-counter model was found to fit the count-rate characteristics of both single MCPs and multi-stage detectors. The model assumed an exponential recovery of gain with time after the MCP had "fired" (an assumption since confirmed by the measurements of Peurrung and Fajans [3], who recorded the MCP gain for the second of two plasma pulses separated by a variable time delay). The properties of an (unspecified) channel recharge circuit were embodied in a parameter k, such that the recharge time constant τ was given by:

$$\tau = kR_{ch}C_{ch} = kR_{MCP}C_{MCP}, \quad (1)$$

where $R_{ch}(C_{ch})$ and $R_{MCP}(C_{MCP})$ are, respectively, the resistance (capacitance) of a single microchannel and of the entire microchannel plate. k is a function of the illuminated area and of the number of multiplier stages.

In this paper we report two successful attempts to extend the dynamic range of an MCP detector.

Most obviously, a reduction in R_{MCP} (Eq. (1)) will improve the count rate capability by reducing channel recharge times. However, the negative temperature coefficient of resistance of the semiconducting channel walls ultimately results in thermal instability as the resistance is reduced. Joule heating in the plate must be counteracted in order to prevent thermal runaway (local melting of the channel matrix). Radiative dissipation alone does not provide stable operation of MCPs at levels of heat generation exceeding 0.1 W cm^{-2}, i.e. for 33 mm diameter plate resistances below ~1 MΩ.

It was previously suggested by one of the authors [4,5] that the output surface of a single plate be bonded directly to a metal anode, which is, in turn, actively cooled ("rear-face" bonding). Conductive heat transfer through the anode can then provide heat dissipation at the required rate. Section 2 below describes our attempts to achieve stable operation of a low resistance, conductivity-cooled MCP (R_{MCP} as low as 260 kΩ at 1320 V) in both rear- and front-cooled configurations. In Section 2.2 we describe a thermal model of such bonded MCPs.

Reduction of R_{MCP} improves high count rate performance by modifying "along-channel" resistance: at the conclusion of our original study [1], we speculated that it might be of interest to also examine a reduction in the "between-channel" resistance provided by the vacuum-evaporated metal electrodes in MCP input and output faces. Section 3 below described a series of count rate measurements made with MCPs bearing a conventional nichrome electrode on one face and a lower-resistivity gold electrode on the opposite face.

* Corresponding author: Tel. +44 116 252 3542; fax +44 116 252 3311; e-mail: gwf@star.le.ac.uk.

PII S0168-9002(96)00482-2

2. Conductively-cooled low resistance MCPs

2.1. Experimental configuration

Three rimless Galileo [6] MCPs (33 mm outer diameter, 10 μm pores, channel length-to-diameter ratio $L/D = 60:1$, 8° bias angle), with extremely low (≤500 kΩ) room temperature resistances were used in our (non-imaging) experiments. Fig. 1 shows the detector assembly used in most tests. A Peltier cooler (Melcor [7], Type CP2-49-06L) was used as a heat sink, with the MCP bonded to a molybdenum anode, and the anode, in turn, glued to the surface of the cooler. Molybdenum was chosen for its low expansion coefficient and reasonably high coefficient of thermal conductivity. The other surface of the cooler was bonded to a 150 mm vacuum flange, which could itself be cooled by water flow through a copper pipe. Auxiliary water cooling of the flange was used in some experiments in order to prevent "heat feedback" in the cooler itself, it being necessary to dissipate the heat generated not only by the microchannel plate, but also by the Peltier cooler.

The most difficult problem we faced was to provide a uniform, efficient thermal contact between the MCP and the anode over the whole MCP surface. We investigated a number of different bonding techniques in order to establish the best thermal conductivity between the microchannel plate and its cooled substrate. Indium bonding [4,5] was not reconsidered.

2.1.1. Epoxy bonding

Initially, the use of conductive adhesive (EPO-TEK 415G, Epoxy Technology [8]) seemed to be a straightforward method of attaching the MCP to the anode. Two attempts to bond one MCP using conductive adhesive (referred to below as Detector 1) were made, followed by resistivity-bias measurements. For these measurements the front (input) electrode consisted of a copper disk, covering the entire area of the MCP. Much attention was given to the uniformity of bonding but the plate never exhibited satisfactory thermal stability, even with the Peltier cooler voltage at maximum (5 V). Fig. 2 shows the dependence of MCP resistance R_{MCP} on the applied bias for Detector 1. Thermal contact between the plate and its cooled substrate appeared to be deficient and the plate suffered "thermal runaway" at a bias of 680 V. The resistance of the plate dropped instantly to zero and pressure in the vacuum chamber rose from 4×10^{-7} to 2×10^{-5} mbar. After the breakdown the plate exhibited a number of ≤0.5 mm diameter black holes and a large discolouration occupying ~25% of the plate surface. Moreover, the plate had several fissures which we attribute to mechanical stresses arising from high local temperature gradients and hot plasma bursts.

Scanning electron microscope (SEM) images of the MCP helped us to understand the reasons for the failure. Despite all efforts to get uniform thermal contact over the plate surface, there were, on inspection, areas where the MCP was not in thermal contact with the anode. However, the main problem in the epoxy bonding was penetration of the liquid epoxy into MCP channels due to surface tension effects. This penetration locally reduced the effective thickness of the plate, decreasing the resistivity of particular channels and led to local heat stresses in the plate. The SEM study revealed that in some channels the epoxy penetrated to nearly half the channel length (see Fig. 3).

2.1.2. Thermoplastic bonding

After the failure of epoxy bonding, a non-liquid adhesive was used – Staystik 171-571 from Alfa Metals Ltd. [9], a thermoplastic film adhesive. The bonding procedure here is very simple: it involves only heating up to 150–200°C and subsequent cooling to room temperature.

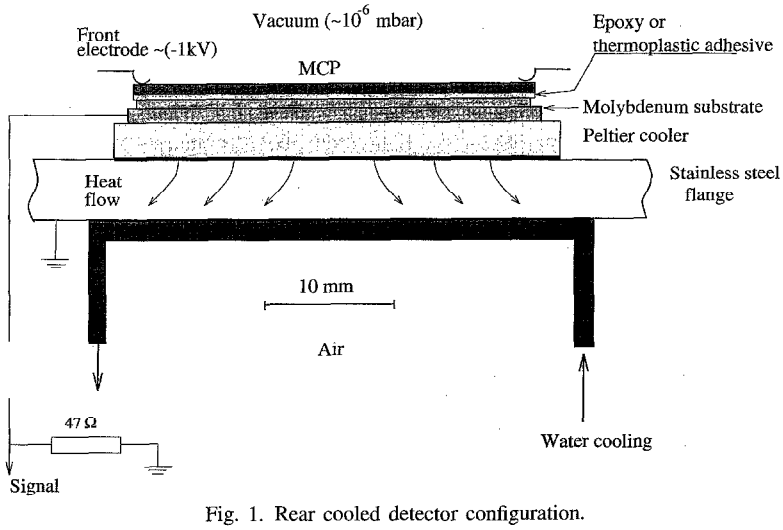

Fig. 1. Rear cooled detector configuration.

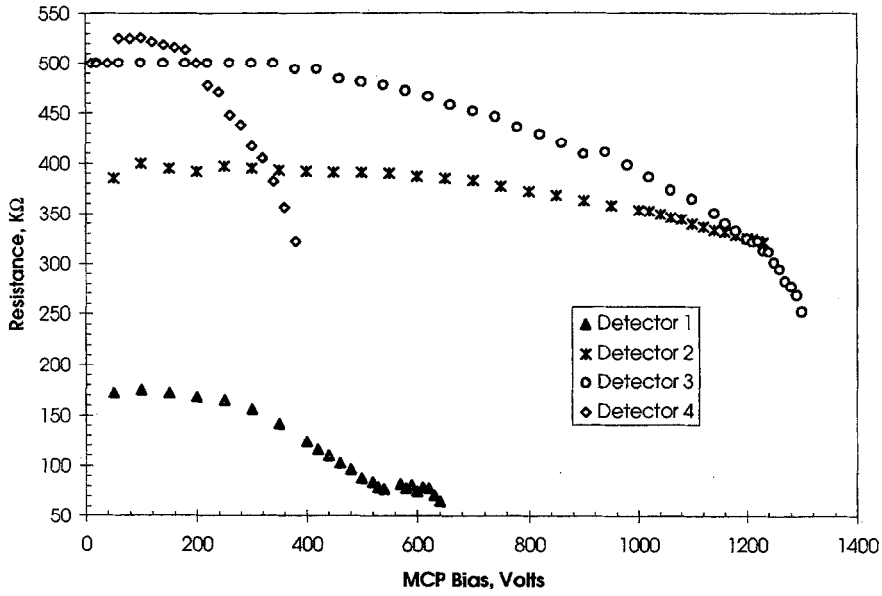

Fig. 2. Variation of MCP resistance with applied bias. ▲ – Detector 1: rear-cooled, liquid epoxy bonding. * – Detector 2: rear-cooled, thermoplastic adhesive bonding. Water cooling of the flange only. ○ – Detector 3: rear-cooled, thermoplastic adhesive bonding. ◇ – Detector 4: front cooled, contact bonding.

Another advantage of this type of adhesive is that it is possible to rebond components by first heating to the same elevated temperatures. A second Galileo MCP was bonded using Staystik to a molybdenum substrate/rear bias electrode/signal collector. Thereafter the substrate was bonded directly to the thermoelectric cooler, again using EPO-TEK 415G epoxy. Two types of front electrode were used for this detector assembly. A copper strip $0.5 \times 4\ cm^2$ was first bonded to the front surface of the plate using the Staystik adhesive (Detector 2). Later, a third MCP was bonded to the same molybdenum substrate using the same staystik process (Detector 3), but with an annular leaf-spring electrode at the front of the assembly.

The thermoplastic adhesive provided an effective and uniform thermal contact as indicated by measurements of the variation of R_{MCP} with applied bias (see Fig. 2). For Detector 2, with only water cooling of the flange and the thermoelectric cooler off, the plate operated stably up to 1230 V, when it suffered thermal runaway. On inspection, the surface of the plate had one region of obvious damage, located in the area where the strip front electrode was bonded to the plate by thermoplastic adhesive. Damage to the plate appeared to be due to the presence of the melted adhesive on its front surface. Radial marks observed on the input surface of the plate, all emanating from the front electrode region, indicated the sputtering of melted adhesive. We conclude that the front surface of the MCP must be kept clean in a rear-cooled configuration and no adhesives can be used for front electrode attachment.

The results of the resistive stability test of Detector 3 are shown in Fig. 2 (circles). This detector reproducibly operated in a stable manner at biases up to 1320 V; count rate measurements, described in Section 2.1.5, were therefore performed with that detector. When the plate finally

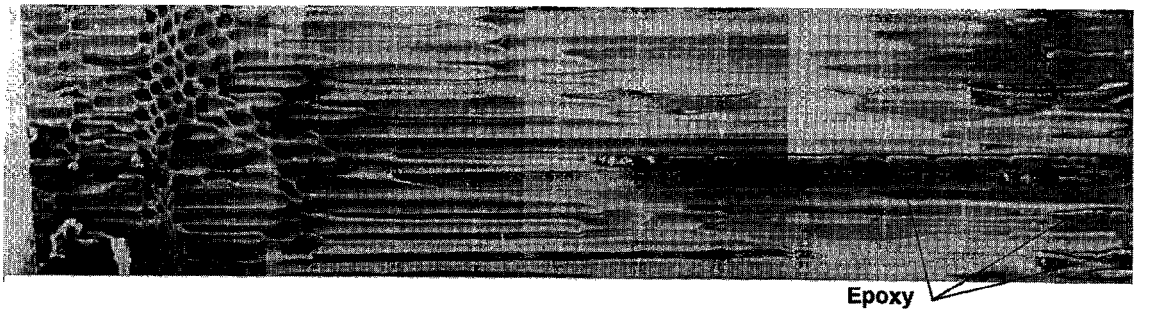

Fig. 3. Scanning electron microscope image of section through liquid epoxy bonded MCP.

(after reproducibly stable operation for several hours at biases ~1300 V) underwent thermal instability, we observed that the only damage region on the MCP was in the place where the annular front electrode (with sharp edges) touched the surface of the plate.

2.1.3. Front-cooled MCP

Attachment of an MCP to an actively-cooled substrate (above) makes it impossible to use conventional MCP readout methods to obtain spatial information. No charge-division or charge-sharing readouts can be used in the rear-cooled geometry. An alternative is to attach the *front* surface of the plate to an actively cooled substrate which is transparent to the radiation to be registered. A sapphire disk, bonded to an annular thermoelectric cooler (Fig. 4) is a possible basis for an imaging front-cooled UV detector. Obviously, any adhesive to be used for bonding the MCP to its sapphire window should also be transparent. For our experiments, we were unable to find a UV transparent adhesive. We therefore tried to mate the MCP to the surface of the sapphire window using mechanical pressure from a rear spring electrode alone (detector 4, shown schematically in Fig. 4). Fig. 2 shows the results of R_{MCP} versus bias measurements for this detector. There was unfortunately poor thermal contact between the plate and the sapphire window. The resistance of the plate had fallen by 36% at a bias of only 380 V, when the experiment was stopped.

2.1.4. Thermalisation

All four detectors exhibited a time-dependent "thermalisation signature" in response to increases in bias. R_{MCP} normally fell abruptly when the bias was increased (i.e. when the rate of Joule heating underwent a step-function increase) and then gradually recovered to a value which was constant over time. The time scale of this recovery depended on the efficiency of heat dissipation from the plate, i.e. on the quality of the thermal contact between the plate and the actively cooled substrate. Detectors 1 and 4 exhibited thermalisation at biases as low as 350 V, while Detectors 2 and 3 showed this response only at biases higher than 900 V. The time for the resistance drop was usually several seconds, while thermalisation took up to tens of minutes.

2.1.5. Count rate measurements

Count rate tests were performed with Detector 3. A pinhole of 0.05 mm^2 area was installed in the detector in order to prevent saturation of the pulse-counting electronics. A mercury vapour UV lamp (2540 Å) was used to illuminate the detector. The obtainable count rate of the detector was unfortunately limited by the maximum intensity of this lamp–pinhole combination and not by the intrinsic characteristics of the plate. The variation of signal and noise count rates with bias applied in presented in Fig. 5. The dark count rate remained below 1.17 $cm^{-2}\,s^{-1}$ while the signal count rate reached 10^8 $cm^{-2}\,s^{-1}$ (~125 counts $channel^{-1}\,s^{-1}$) at a bias of 1300 V. Both signal and pulse height distributions were quasi-exponential (see Fig. 6). The linear dependence of the UV count rate on the bias applied (Fig. 5) indicates that there was no recharge current limitation of the count rate capabilities of this MCP and suggests that much higher values of count rate could have been achieved with brighter illumination. Further indirect evidence for this possibility lies in the ratio of pulse current I_p to conduction (strip) current I_s [1,2]. At the highest measured count rate (10^8 $cm^{-2}\,s^{-1}$), the ratio I_p/I_s was only 1.5×10^{-3}, which is more than two orders of magnitude lower than the asymptotic (illuminated-area-independent) limiting value for a single MCP which is

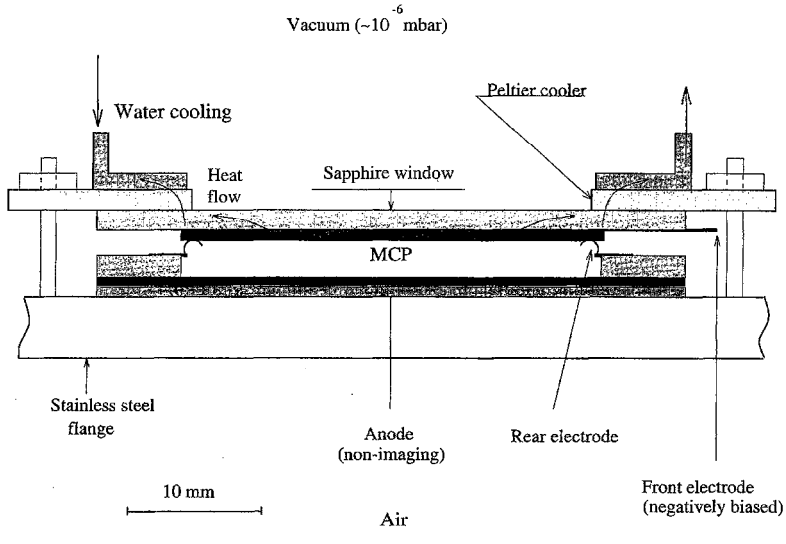

Fig. 4. Front cooled detector configuration.

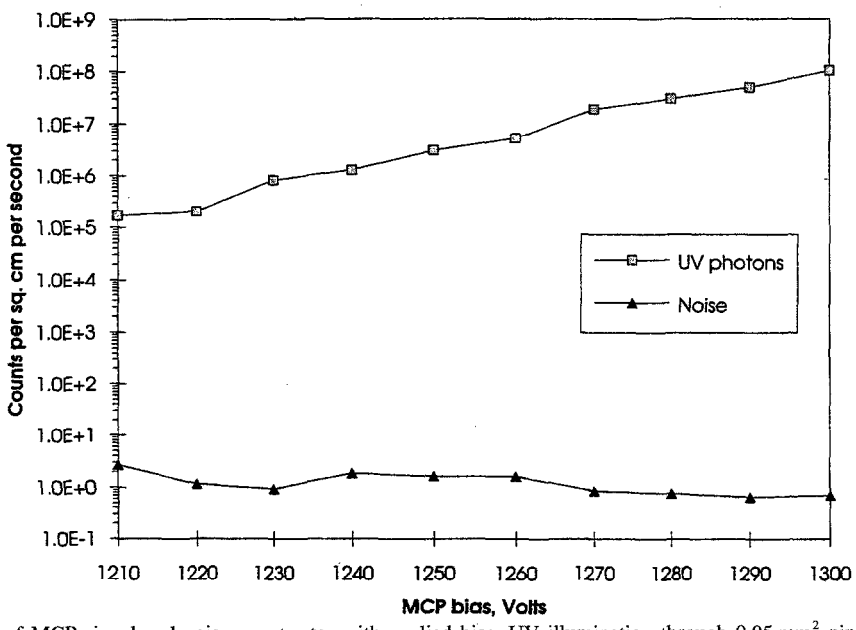

Fig. 5. Variation of MCP signal and noise count rates with applied bias. UV illumination through 0.05 mm^2 pinhole, Detector 3.

0.48 as deduced in Ref. [1]. The inference is that Detector 3 would have been capable of count rates equivalent to $\sim 3 \times 10^{10}\,cm^{-2}\,s^{-1}$ had a sufficiently bright source of excitation been available.

We observed also a decrease of plate resistance when the UV lamp was switched on at a bias of 1300 V. The resistance dropped from 264 to 263 kΩ and recovered in about 30 s after the light was switched off. This resistance drop is likely to be due to the local heating of the active area by the strip current.

2.2. Thermal modelling of bonded MCPs

2.2.1. One-dimensional model

We constructed a thermal model of a conductively cooled MCP to provide a basis for a better understanding

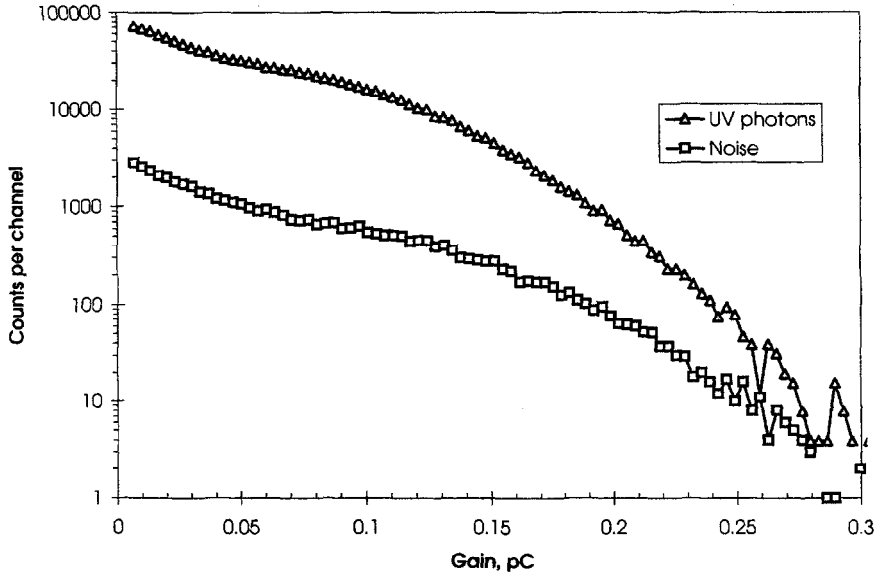

Fig. 6. Signal and noise pulse height distributions. Detector 3, UV illumination, bias 1300 V. Lower discriminator level ~0.01 pC. Signal and noise count rates $10^3\,cm^{-2}\,s^{-1}$ and $30\,cm^{-2}\,s^{-1}$, respectively.

of MCP thermal behaviour and to allow the estimation of critical operational parameters, in particular, maximum tolerable bias voltage. A previous numerical model of bonded MCPs [4,5] showed that the temperature difference across a low-resistance plate ($R_{MCP} = 10^5\ \Omega$, $L/D = 40:1$, 10 μm pores) with heat dissipation of 1–10 W is only several tens of degrees. These studies assumed that the MCP resistance depended only on the plate temperature, viz:

$$R_{MCP}(T) = R_0(1 - \alpha(T - T_0))$$

as suggested in Ref. [10]. The rear surface of the plate was assumed to be held at a constant temperature T_0 (T_0 is the substrate temperature) by conductive cooling. The calculated variation of R_{MCP} with applied voltage was not in a good agreement with our measurements; the model was therefore further developed on the basis of the new data.

A recent study of MCP resistance in a temperature controlled environment revealed a linear decrease of R_{MCP} with both MCP temperature and applied high voltage [11]:

$$R_{MCP}(T) = R_0(1 - \alpha_T(T - T_0) - \alpha_V V)\,. \tag{2}$$

As reported in Ref. [12], the time variation of MCP resistance with voltage may be caused by an electrolysis mechanism initiated by water vapour absorbed on the channel surfaces. According to that model, the voltage dependence may become weaker with time spent in vacuum. The time variation of R_{MCP} was not investigated in Ref. [11]. As in Refs. [4,5], we first assumed (and verified by later calculations) that the temperature variation across the channel wall is negligible, i.e. the plate temperature varies only along the channel length (the x-axis). We define $x = L$ to be the MCP input surface, and $x = 0$ to be the output (rear-cooled) side in contact with the substrate. The heat conduction equation in our case is then expressed as follows:

$$\frac{\partial^2 T}{\partial x^2} + \frac{\dot{q}(t,x)}{K} = \frac{1}{\alpha}\frac{\partial T}{\partial t}\,, \tag{3}$$

$$\dot{q}(t,x) = I^2(t) r(t,x)/A^2\,, \tag{4}$$

$$I(t) = V_{MCP} A \left[\int_0^L r(t,x)\,dx\right]^{-1}\,, \tag{5}$$

$$A = \frac{\pi D_0^2}{4}(1 - A_{open})\,, \tag{6}$$

$$\alpha = K/c_p\rho\,. \tag{7}$$

Here, K is the thermal conductivity, ρ the MCP glass density, c_p the thermal capacity, r the glass resistivity, V_{MCP} the bias applied, L and D_0 are the MCP thickness and diameter and A_{open} is the MCP open area fraction. Using Eq. (2), the resistivity function $r(t,x)$ can be expressed as follows:

$$r(t,x) = \frac{r_0(1 - \alpha_T(T(t,x) - T_0))}{1 + \alpha_V I(t) r_0 L/A}\,. \tag{8}$$

We arrive at the following equation:

$$\frac{\partial^2 T}{\partial x^2} + \frac{I^2(t)}{KA^2}\frac{r_0(1 - \alpha_T(T(t,x) - T_0))}{1 + \alpha_V I(t)\cdot r_0 \cdot L/A} = \frac{1}{\alpha}\frac{\partial T}{\partial t}\,; \tag{9}$$

which has to be solved together with Eq. (5).

The radiation formula

$$Q_{Rad} = \frac{\pi D_0^2}{4}\sigma\varepsilon(T_{MCP}^4 - T_A^4)\,,$$

where [13] σ is Stefan's constant, T_A the laboratory ambient temperature, T_{MCP} the temperature of the radiating MCP surface ($x = L$ in order case of rear-cooled configuration), ε the effective thermal emittance ($\varepsilon = 0.4$, [10]), yields an estimate for heat dissipation from the MCP of only 0.015 W cm^{-2} for $T_{MCP} = 70°$. Therefore, in our case, the rate of conductive cooling must dominate over the radiative cooling through the open surface of the plate and the channel walls. The boundary condition on the open side of the plate ($X = L$) is then:

$$\partial T/\partial x = 0\,. \tag{10}$$

In the case of ideal bonding the temperature of the cooled surface ($x = 0$) is constant at a level T_0, the temperature of the substrate. However, if not the whole surface of the MCP is in ideal thermal contact with the substrate, there is temperature variation over the MCP–substrate inference. A convection-like boundary condition with the average temperature of the cooled surface T is more appropriate at $x = 0$:

$$-K\frac{\partial T}{\partial x} = h(T - T_0)\,, \tag{11}$$

where the coefficient h represents the quality of bonding.

The solution of Eqs. (5) and (9) subject to boundary conditions (10) and (11) can be obtained numerically using an iterative procedure. On each iteration step it is necessary to calculate the current $I(t)$ and then solve the partial differential equation with the current fixed.

2.2.2. Results

The family of equations above contains a parameter h, representing the "quality" of MCP bonding, which can be determined for each particular detector by fitting to the measured variation of MCP resistance with bias applied (see Fig. 7). For the rear-cooled detector with thermoplastic bonding (Detector 3) a value of $h = 0.0881$ W C^{-1} cm^{-2} gives the best fit, with parameter values: $D_0 =$ 33 mm, $A_{open} = 63\%$, $L = 600$ μm. A temperature coefficient of resistance value $\alpha_T = 0.015$ C^{-1} was taken from Ref. [10]; the voltage coefficient of resistance value $\alpha_V = 6 \times 10^{-5}$ V^{-1} from Ref. [11]. We used the standard MCP

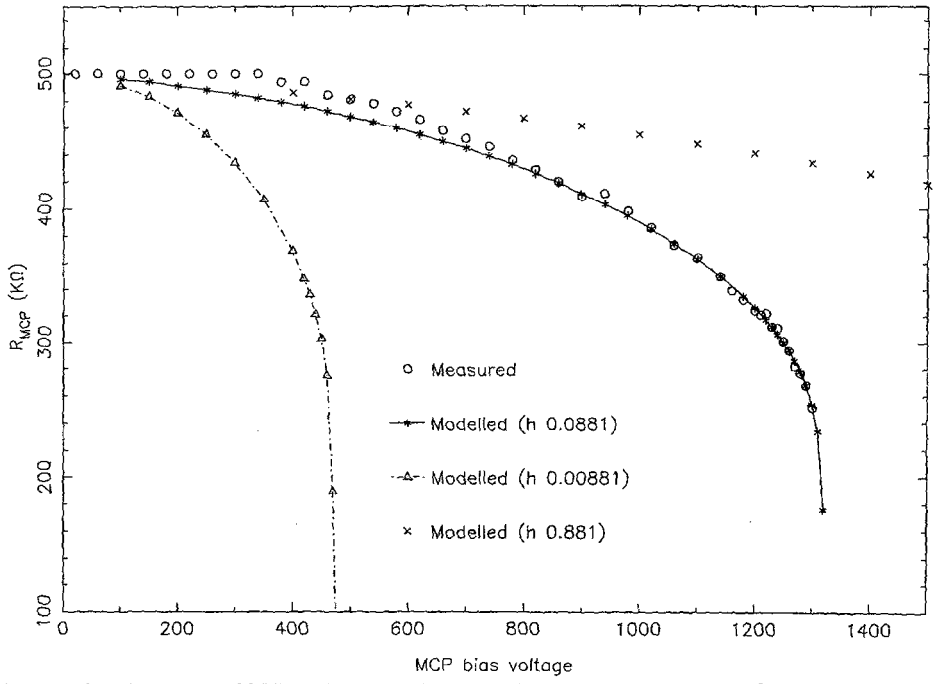

Fig. 7. Measured and modelled variation of MCP resistance with bias applied, Detector 3. $R_0 = 500$ kΩ, $L/D = 60:1$, 10) μm pores, MCP diameter 33 mm, $A_{open} = 63\%$. Conductively cooled rear surface. Bonding coefficient $h = 0.0881$ (stars), 0.00881 (triangles) and 0.881 (crosses) W C^{-1} cm^{-2}.

glass values for $\rho c_p = 1.8$ J cm^{-3} C^{-1} and $K = 1.1 \times 10^{-2}$ W cm^{-1} C^{-1} [11,13,14].

Fig. 7 shows that, in theory and in practice, a bias voltage of 1320 V constitutes the operational limit for Detector 3 as R_{MCP} drops very rapidly at higher biases. The results of the model are in good agreement with the

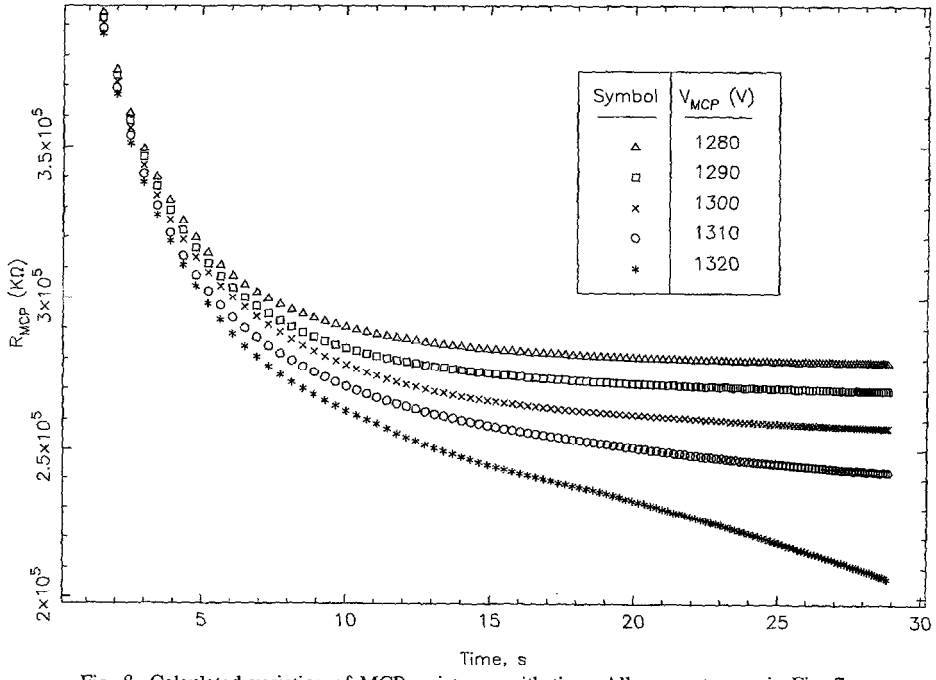

Fig. 8. Calculated variation of MCP resistance with time. All parameters as in Fig. 7.

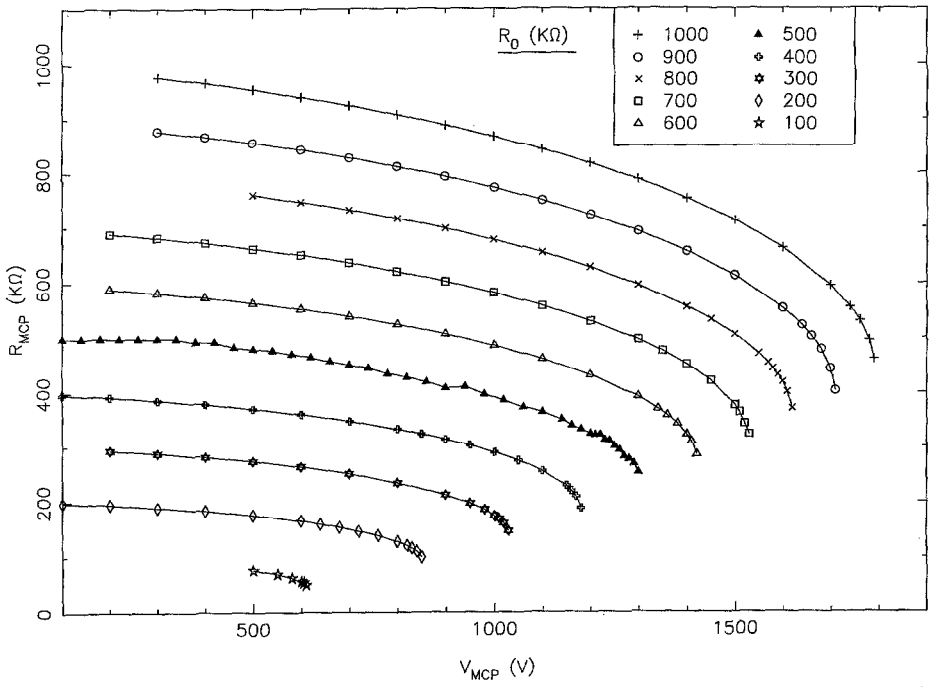

Fig. 9. Calculated variation of MCP resistance with applied bias for different values of R_0. All parameters as in Fig. 7.

experimental data. Fig. 8 shows the calculated time variation of R_{MCP} for Detector 3 at 1280, 1290, 1300, 1310 and 1320 V. At biases below 1310 V the MCP resistance becomes stable with time, corresponding to a state of thermal equilibrium between heat generation in MCP and the heat conducted out by the substrate. Cooling is insufficient at higher biases and the resistance starts decreasing linearly with time. The modelled temperature

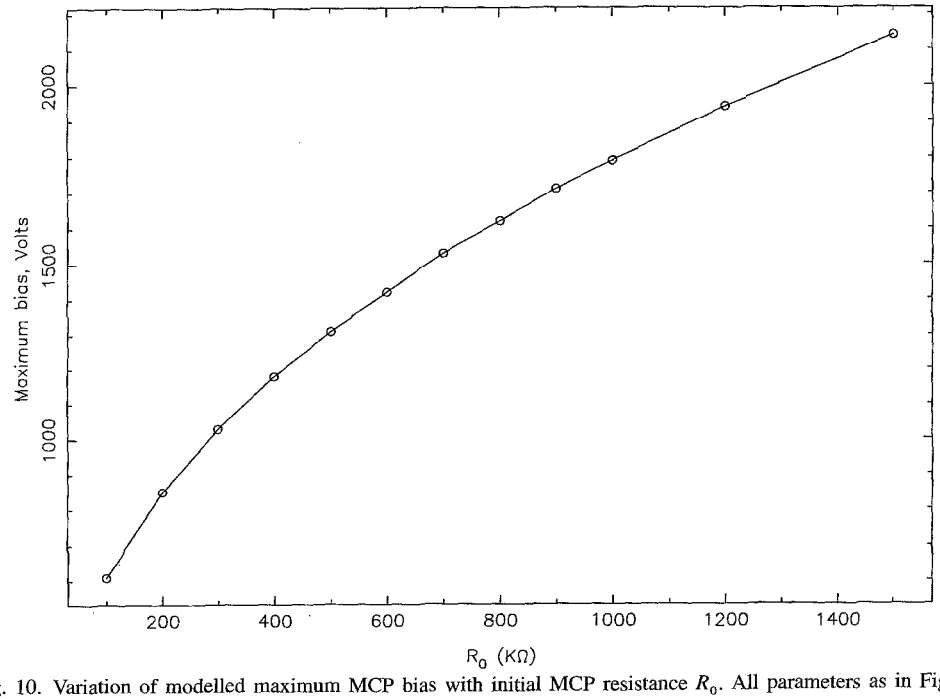

Fig. 10. Variation of modelled maximum MCP bias with initial MCP resistance R_0. All parameters as in Fig. 7.

difference along the length of the channels in Detector 3 was no higher than 10° at biases lower than 1310 V, while the difference between the average temperature of the rear surface and the cooling substrate was about 20°. The most pronounced temperature variation is observed in the part of the channel adjacent to the substrate ($x = 0$ in our case), as reported in Ref. [5].

Having tested our model by comparison with the measured data, we can use it to estimate maximum operating voltages for a range of zero-bias MCP resistances. Fig. 9 shows the results of modelling MCPs with different initial (zero-bias) resistances assuming that the quality of bonding, defined by the coefficient h, is the same as in Detector 3. These calculations are summarised in Fig. 10, which shows how the maximum bias (at which the MCP achieves thermally stable operation) varies with the initial resistance of the plate, R_0. A single MCP of $L/D = 60:1$ ideally requires a bias voltage of 985 V for acceptable pulse-counting operation [15]. We see from Fig. 10 the minimum acceptable value of R_0 is 300 kΩ, i.e. Detector 3 should have had a substantial safety margin for operation. Fig. 5, however, indicates that at least 1200 V was required to give measurable output and that the gain of microchannels sealed at one end may be substantially less, at a given voltage [16], than those of conventionally-operated MCPs.

3. MCP with gold electrodes

Two MCPs with one face bearing a gold electrode and the other with a regular nichrome layer were received from Philips Photonics [17] and used to investigate the dependence of MCP count rate capability on electrode type. The degree of electrode penetration ("endspoiling") into the channels was a standard one channel diameter, for both gold and nichrome.

Based on simple deposition on glass slides, the MCP manufacturer claims surface resistances for gold and nichrome electrodes of 10 and 150 Ω/□, respectively [18]. This gold-to-nichrome resistance ratio is greater than would be expected from a simple ratio of resistivities (1:40). We note first, that gold evaporation onto glass requires a thin (~100 Å) "key" layer of nichrome to make the gold stick. Secondly, Katayama et al. [19] have performed an equivalent circuit analysis of MCP electrodes, showing that:

$$(R_{\square})_{\text{electrode}} = \frac{p}{(0.866p - D)} (R_{\square})_{\text{metal}}, \tag{12}$$

where p, D are the inter-channel pitch and channel diameter respectively and $(R_{\square})_{\text{electrode}}$ and $(R_{\square})_{\text{metal}}$ are, respectively, the surface resistances, for a common layer thickness t, of the MCP electrode and of its constituent metal in the form of a continuous surface. For $p = 15$ μm, $D = 12.5$ μm, appropriate to our Philips plates:

$$(R_{\square})_{\text{electrode}} \simeq 30(R_{\square})_{\text{metal}}, \tag{13}$$

where, assuming a nichrome thickness $t = 1000$ Å, and a nichrome resistivity $\sim 10^{-4}$ Ω cm, we obtain an estimate of 300 Ω/□ for the surface resistance of the nichrome faces of the test MCPs (referred to below as MCPs 1 and 2) – slightly higher than the manufacturer's estimate given above.

By changing the plate orientation in the MCP stack we varied the type of electrode on both input and output surfaces of both front and rear MCPs, with the other assembly parameters fixed. Fig. 11 summarises the detector assemblies ("Modes") used in our measurements. In Modes D, D1, E and E1 we used a third Philips MCP of the same geometry (MCP3) with resistance $R_{\text{MCP}} = 1200$ MΩ and nichrome electrodes on both input and output faces. The availability of this plate allowed us to

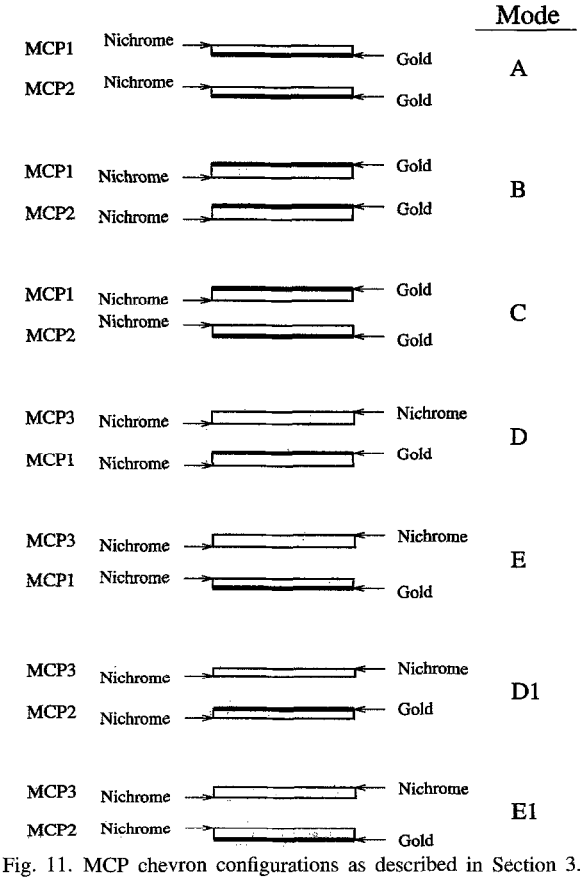

Fig. 11. MCP chevron configurations as described in Section 3. Each plate was 36 mm in diameter with 12.5 μm pores, length to diameter ratio $L/D = 80:1$, measured resistance $R_{\text{MCP}} \sim 500$ MΩ, open area fraction $A_{\text{open}} = 63\%$, channel density 5100 pores mm^{-2} and channel bias angle 13°.

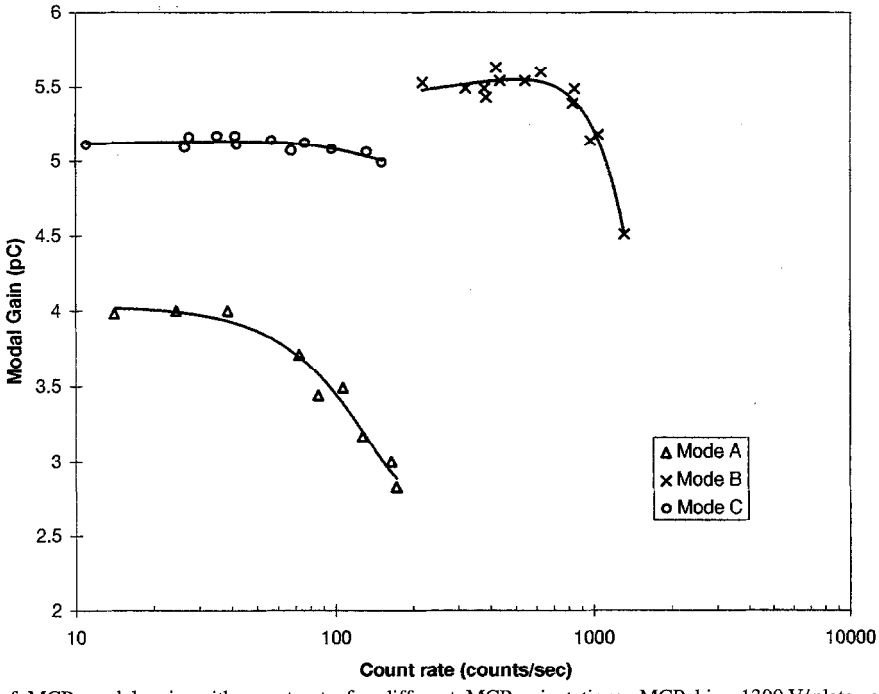

Fig. 12. Variation of MCP modal gain with count rate for different MCP orientations. MCP bias 1300 V/plate, electron-accelerating inter-plate gap voltage 200 V. △ – Mode A, Gold coating on the MCP output surfaces. × – Mode B, gold coating on the MCP input surfaces. ○ – Mode C.

test differences in MCP performance independently on both plates MCP1 and MCP2. For all detector modes A–E1 count rate measurements were made using 2540 Å UV illumination through the same image mask positioned 4.5 mm in front of the input plate. The mask contained a number of pinholes of 0.1 mm in diameter, all, except the central one, covered by photographic film. The illuminated area corresponds to ~100 channels. Count rate measurements for Modes A, B, C are presented in Fig. 12.

The detector assembly B exhibited substantially better count rate performance than Modes A and C. The gain of the detector was significantly higher with the gold electrode serving as the input surface (Mode B), than for the reverse orientation of the plates, Mode A. Furthermore,

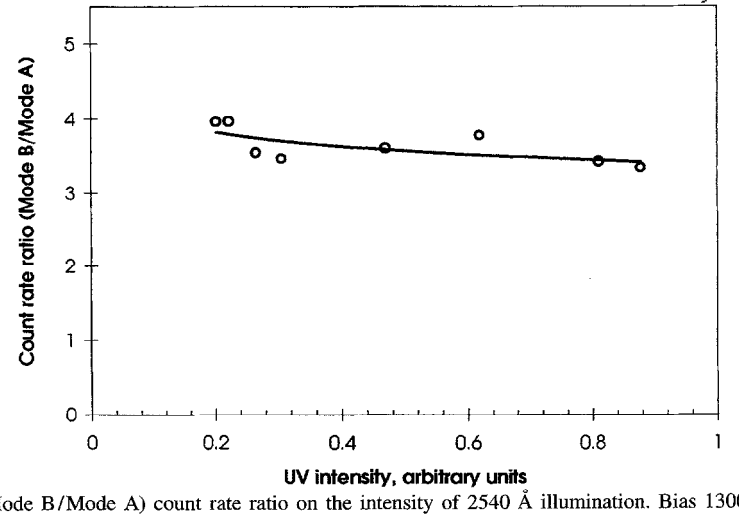

Fig. 13. Dependence of (Mode B/Mode A) count rate ratio on the intensity of 2540 Å illumination. Bias 1300 V/plate. The fact that the ratio is greater than unity reflects the higher quantum efficiency of gold for UV light, compared to nichrome.

was observed that the quantum detection efficiency of Modes B and C (a factor of ~3.6 in the former case) was substantially higher than for the assembly in Mode A (see Fig. 13).

We conclude that gold coating of the *input* surface of an MCP does improve the plate characteristics as compared to conventional nichrome coating as (speculatively) hypothesised in Ref. [1]. Since the replacement current, which reestablishes the electric field in "fired" channels, flows from the input (low voltage) surface of the MCP to the output surface, it is indeed plausible that changing the input nichrome electrode to gold should have the

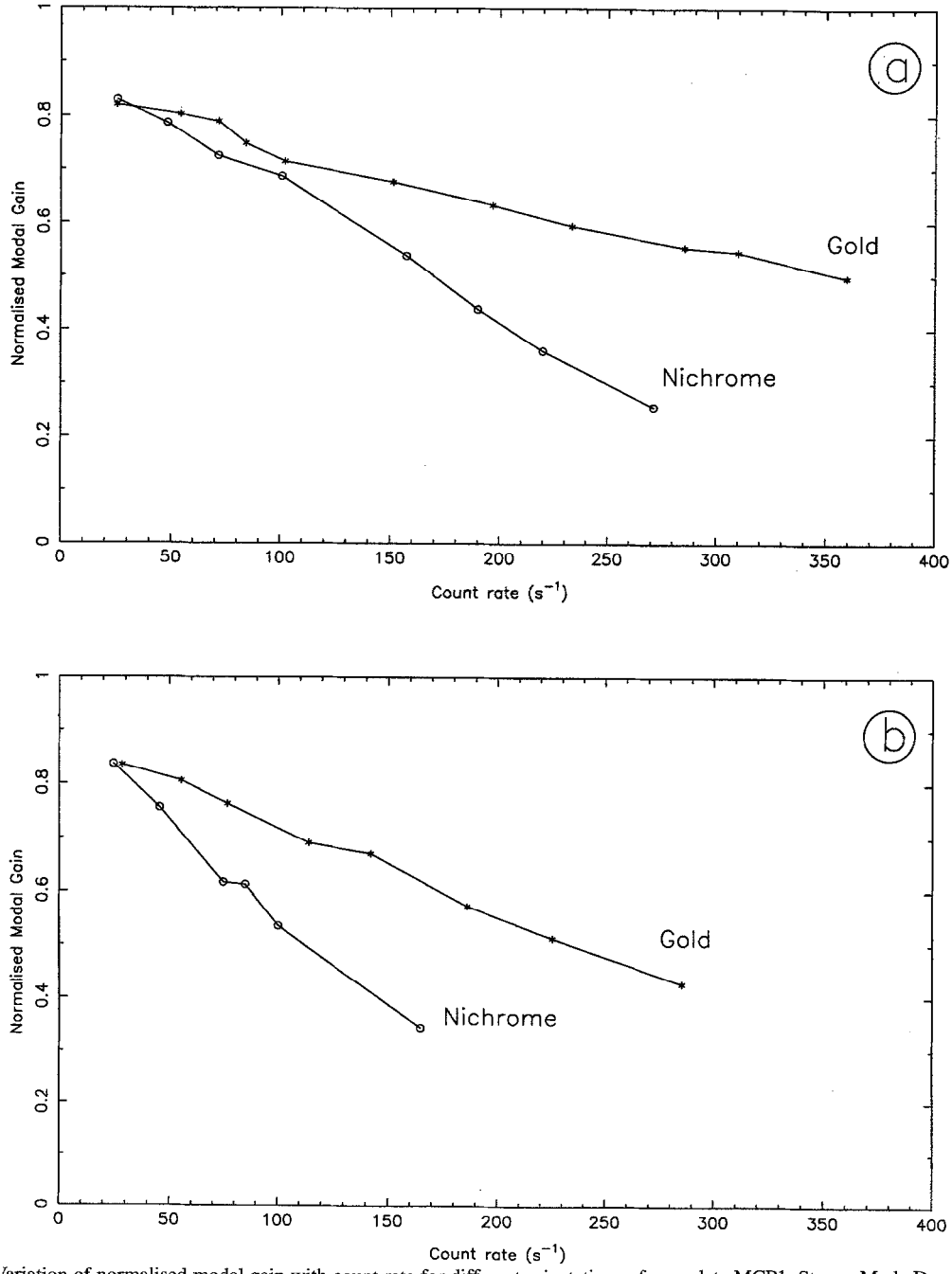

Fig. 14. (a) Variation of normalised modal gain with count rate for different orientations of rear plate MCP1. Stars – Mode D, gold electrode as input face. Circles – Mode E, nichrome electrode as input face. (b) As (a), for rear plate MCP2, Modes D1 and E1.

most significant effect. Since conduction in MCPs is by means of a sub-surface semiconducting lead layer overlaid by a silica skin [20], it may be that the reason for the improved count rate capability of Au-electroded MCPs arises, not simply from their lower electrode resistivity, but from the precise details of the metal–glass interface.

We proceeded with Modes D and E in order to test the influence of electrode type on the count rate characteristics of plates MCP1 and MCP2 independently. MCP3 was used as the front plate in these assemblies. The gains of detector Modes E and E1, with the gold coating serving as the output surface, were, as expected from the results obtained with Modes A–C, lower, at a given count rate, that the gains of detector Modes D and D1. The maximum available count rate was limited by the high resistance front plate and we observed a quasi-linear fall in gain with increase of count rate. However, the rate of that gain decrease was different for the two orientations of MCP1 and MCP2. As can be seen in Fig. 14, gold coating the input surface of the rear plate in the chevron for both MCP1 and MCP2 (Modes D and D1) showed better count rate capabilities than the equivalent assemblies with nichrome in that critical position, Modes E and E1.

4. Conclusions

The results of our tests with low-resistance conductively-cooled microchannel plates showed the possibility of increasing the count rate characteristics of MCP detectors by using plates with a much lower than normal resistance. We managed to find an effective way of reproducibly and stably operating MCPs ($L/D = 60:1$, 10 μm pores) at biases up to 1320 V in the rear-cooled configuration, when the ohmic heating reached the level of 0.78 W cm^{-2}. Although we were not able to achieve count rate values higher than 10^8 cm^{-2} s^{-1} due to the low intensity of incoming radiation, the channel recharge time was some tens of μs and the detector limit may have been as high as 3×10^{10} cm^{-2} s^{-1}. The bonding procedure of the MCP to the cooled substrate is very simple and does not require any specialised equipment. We have shown that liquid epoxies cannot be used for attaching the MCP to its substrate, since the epoxy can penetrate the channels due to surface tension effects. Cooling of the MCP input face was unsuccessful as the thermal contact between the plate and the actively cooled substrate was not sufficient, although the use of a radiation-transparent epoxy for that bonding method could possibly lead to high count rate capabilities in front-cooled imaging detectors.

The results of our thermal modelling allowed us to estimate the lowest initial MCP resistance for given MCP geometry and applied bias.

Investigation of MCP capabilities for two different types of electrode coating revealed that gold-coated plates exhibited much better count rate characteristics in comparison with conventional nichrome-coated MCPs. Moreover, gold-electroded plates have higher output gain and UV quantum detection efficiency. It was shown that the input surface coating is the most critical for the count rate characteristics, as well as for the output gain. The characteristics of a detector assembly comprising two ~500 MΩ MCPs with gold-coated input faces remained constant up to a count rate value of ~18 counts ch^{-1} s^{-1} (compared to the count rate 125 counts ch^{-1} s^{-1} obtained with the bonded ~500 kΩ MCP of Detector 3).

Acknowledgements

This work reported here on bonded MCPs was supported by NSF Award No. DMI-9461065. The authors sincerely thank J.E. Spragg for his help with MCP bonding and Dr. G. McTurk for obtaining the SEM image shown in Fig. 3. AST gratefully acknowledges the receipt of a Royal Society Fellowship and support from Nova Scientific. The work of Leicester X-ray Astronomy Group is supported by the UK PPARC, who provided a Research Fellowship for JFP.

References

[1] G.W. Fraser, M.T. Pain, J.E. Lees and J.F. Pearson, Nucl. Instr. and Meth. A 306 (1991) 247.
[2] G.W. Fraser, M.T. Pain and J.E. Lees, Nucl. Instr. and Meth. A 327 (1993) 328.
[3] A.J. Peurrung and J. Fajans, Rev. Sci. Instr. 64 (1993) 52.
[4] W.B. Feller, Proc. SPIE 1243 (1990) 149.
[5] W.B. Feller, Nucl. Instr. and Meth. A 310 (1991) 249.
[6] Galileo Electro-Optics, Galileo Park, Sturbridge, MA 01566, USA.
[7] MELCOR Corporation, 1040 Spruce Street, Trenton, NJ 08646, USA.
[8] Epoxy Technology, Inc., 14 Fortune Drive, Billerica, MA 01821-3972, USA.
[9] Alfa Metals Ltd., 1, The Broadway, Tolworth, Surbiton, Surrey, KT6 7DQ, England.
[10] J.F. Pearson, G.W. Fraser and M.J. Whiteley, Nucl. Instr. and Meth. A 258 (1987) 270.
[11] A. Sardella, M. Bassan, L. Guidicotti, L. Lotto and R. Pasqualotto, Proc. SPIE 2551 (1995) 273.
[12] J.P. Rager and J.F. Renaud, Rev. Sci. Instr. 45 (1974) 922.
[13] P.B. Soul, Nucl. Instr. and Meth. 97 (1971) 555.
[14] D.C. Slater and J.G. Timothy, Rev. Sci. Instr. 64 (1993) 430.
[15] G.W. Fraser, J.F. Pearson, G.C. Smith, M. Lewis and M.A. Barstow, IEEE Trans. Nucl. Sci. NS-30 (1983) 455.

[16] P.W. Graves, B.D. Klettke, N.D. Krym and W.G. Wolber, Bendix Electro-Optics Division, Technical Applications Note 6902 (1969).
[17] Philips Photonics, B.P. 520, Avenue Roger Roncier, Brive la Gaillarde Cedex, F19106 France.
[18] J. Smith, Philips Photonics, private communications (1992).
[19] M. Katayama, M. Nakai, T. Yamanaka, Y. Izawa and S. Nakai, Rev. Sci. Instr. 62 (1991) 124.
[20] J.J. Fijol, A.M. Then, G.W. Tasker and R.J. Soave, Appl. Surf. Sci. 48/49 (1991) 464.